Role of electron-phonon interaction on quasiparticle dispersion in the strongly correlated cuprate superconductors

R. Citro
Dipartimento di Fisica "E. R. Caianiello" and C.N.I.S.M., Università degli Studi di Salerno, Via S. Allende, I-84081 Baronissi (Sa), Italy

S. Cojocaru
Dipartimento di Fisica "E. R. Caianiello" and C.N.I.S.M., Università degli Studi di Salerno, Via S. Allende, I-84081 Baronissi (Sa), Italy and Institute of Applied Physics, Chisinau 2028, Moldova

M. Marinaro
Dipartimento di Fisica "E. R. Caianiello" and C.N.I.S.M., Università degli Studi di Salerno, Via S. Allende, I-84081 Baronissi (Sa), Italy and I.I.A.S.S., Via G. Pellegrino, n. 19 84019 Vietri sul Mare (SA), Italy

(Received 15 June 2005; revised manuscript received 14 December 2005; published 31 January 2006)

The role of the electron-phonon (el-ph) interaction in high-T_c cuprates is investigated theoretically by considering correlated electrons interacting with Holstein phonons within the two-dimensional single-band Hubbard model in the limit of large Coulomb interaction. It is shown that the electron-phonon interaction gives rise to a kink in the dispersion along the nodal direction and to a peak/dip/hump structure in the one-electron spectral weight whose dependence on temperature, isotope substitution, and doping is discussed in relation to recent photoemission experiments on the nodal quasiparticles in Bi2201 and LSCO. A comparison with these experiments shows that electron correlations play a crucial role in the determination of the kink position, size, and doping dependence. We also show that the "unusual" oxygen isotope shift in the real part of the self-energy, experimentally observed in the optimally doped Bi2212 samples, can be qualitatively explained within the framework that incorporates both strong electron correlations and the adiabatic electron-phonon interaction.

DOI: 10.1103/PhysRevB.73.014527 PACS number(s): 74.72.Hs, 71.38.−k, 71.27.+a, 71.10.Fd

I. INTRODUCTION

Understanding the role of the many-body interactions in high T_c cuprates remains an essential step towards the comprehension of the superconductivity in these systems. In recent years angle-resolved photoemission spectroscopy (ARPES) has provided an essential way to probe the coupling of quasiparticles (QP) among themselves and to collective modes.[1,2] ARPES experiments have revealed several intriguing features in the dispersion, weight, and line shape of the quasiparticles. Specifically: (a) a kink in the dispersion in both the nodal and antinodal regions;[3–7] (b) a double peak structure and a dip (peak/dip/hump) in the energy distribution curves (EDCs) along the nodal direction below and above the critical temperature;[7,8] (c) a definite and strong isotope effect[9] in the optimally doped Bi2212 samples at the three different stages of the isotope substitution loop $O^{16} \rightarrow O^{18} \rightarrow O^{16}$. Surprisingly, these isotope effects mainly appear in broad high-energy humps, commonly referred to as "incoherent peaks." These features, especially (a), imply that electrons are coupled to a collective mode. So far, two collective modes, the spin resonance at 41 meV (Refs. 6 and 11–13) and the ~40 meV and ~70 meV phonons[3,7,14–16] have been mainly suggested to explain experiments. Which one is responsible for the kink in the quasiparticle dispersion is still a matter of debate. The major difference between the two proposed scenario lies in their normal state behavior. In the case of phonons a well-defined energy scale in the normal and superconducting state is needed, while in the case of resonance mode scenario, no energy scale is defined in the normal state. The recent experiments on the normal state of Bi2201 and LSCO along the diagonal direction[7,17] provide evidence of an energy scale, i.e., a kink in the energy dispersion, over the entire doping range that persists well above the critical temperature, up to ten times T_c. These results, together with the observation of isotope effects, put a strong constraint on the fundamental scattering process of cuprates[18] supporting a picture where phonons are strongly involved. However, some puzzling features still remain to be explained. On one hand, the low energy electronic dispersion shows a strong concentration dependence at low hole doping that almost saturates close to optimal doping.[14] At the same time, spectral density and dispersion at energy scale larger than the kink are very sensitive to temperature, isotope substitution and doping. In this situation the attempt to describe this experimental scenario within a conventional el-ph framework appears important.

From the theoretical point of view some authors have stressed the importance of the interplay between the electron-phonon coupling and the strong Coulomb interaction within single band Hubbard model[19–26] and t-J model,[27–29] while others have been focused on the analogies and differences between the coupling of quasiparticles to a magnetic π-resonant mode and phonons.[30–32] In our opinion the coexistence of the electron-phonon and strong Coulomb interactions deserves more attention, so in the present paper we investigate in some detail, whether and to what extent, the presence of strong electron correlations modifies the results of the usual adiabatic theory of electron-phonon interaction. Specifically, our study will be focused on the behavior of

nodal quasiparticles once the strong electron correlations are taken into account. To such purpose, we derive below the electron self-energy due to the electron-phonon interaction in a two-dimensional model in which electrons, renormalized by strong Coulomb correlations, interact with a dispersionless optical phonons and discuss the effect of the electron-phonon interaction on the quasiparticle dispersion and line shape in the normal phase.[33]

We consider the Hamiltonian of the Hubbard-Holstein model which is given by

$$H = H_e + H_{e\text{-}p} + H_p, \tag{1}$$

where

$$H_e = \sum_{\langle i,j\rangle,\sigma} t_{ij} c^\dagger_{i\sigma} c_{j\sigma} - \mu \sum_\sigma n_{i\sigma} + U \sum_i n_{i\uparrow} n_{i\downarrow},$$

$$H_{e\text{-}p} = g \sum_{i\sigma} q_i n_{i\sigma},$$

$$H_p = \hbar\,\omega_0 \sum_i \left(b^\dagger_i b_i + \tfrac{1}{2}\right), \tag{2}$$

$c^\dagger_{i\sigma}(c_{i\sigma})$ is an electron creation (annihilation) operator with spin σ at site i, t_{ij} is the nearest neighbor hopping, μ is the chemical potential, $b^\dagger_i(b_i)$ is a phonon creation (annihilation) operator, U is the local Coulomb interaction, $q_i=(1/\sqrt{2})(b^\dagger_i + b_i)$, $n_{i\sigma}=c^\dagger_{i\sigma}c_{i\sigma}$.

It is well known that the Hubbard model describes a variety of physical regimes and phases in correspondence of different values of the parameters. In the present paper we focus on the strong correlated regime $U/W \gg 1$ (where W is the bandwidth) and consider electron concentration $n<1$. Besides, the phonon frequency ω_0 is taken smaller than the bandwidth ($\omega_0/W \ll 1$), and we consider the adiabatic regime. In this regime it appears as a good starting point to compute the electron Green's function in the presence of el-ph interaction and el-el correlations by considering the following expression for the electron self-energy:[38]

$$\Sigma^p_\sigma(\mathbf{k}, i\Omega) = \frac{g^2}{\beta} \sum_{\omega_n} \int \frac{d^2q}{(2\pi)^2} D^0(\mathbf{q}, i\omega_n) G^I_\sigma(\mathbf{k}+\mathbf{q}, i\Omega + i\omega_n), \tag{3}$$

where D^0 is the phonon Green's function and the single particle electron Green's function G^I is approximated by the Hubbard-I solution,

$$G^I_\sigma(\mathbf{k}, i\omega) = [(G^0_\sigma(i\omega))^{-1} - \epsilon_{\mathbf{k}}]^{-1}, \tag{4}$$

with $G^0_\sigma(i\omega)$ being the atomic Green's function

$$G^0_\sigma(i\omega) = \frac{1-\langle n_{-\sigma}\rangle}{i\omega+\mu} + \frac{\langle n_{-\sigma}\rangle}{i\omega-(U-\mu)}. \tag{5}$$

For the square lattice $\epsilon_{\mathbf{k}}=-2t(\cos k_x + \cos k_y)$ and $\langle n_{-\sigma}\rangle$ is the average number of particles with spin $-\sigma$. The approximation (4) for the electron Green's function corresponds to the mean-field level of the strong coupling perturbation theory[34,35] and allows us to describe the main effect of a large, concentration dependent, single-particle spectral weight transfer to high energy ($\sim U$) in the presence of electron correlations. Let us remark that in the regime of strong electron concentration and for electron concentration $n<1$ more accurate approximations, like Dynamical Mean Field Theory (DMFT),[36] predicts a "coherent" quasiparticle peak at the top of the incoherent lower Hubbard band that becomes narrower in the low-doping regime. In Eq. (3) we use the Hubbard-I approximation as an averaged description of both the coherent and incoherent components of the spectrum. Such description is justified in the strong coupling regime away from half-filling.[37] Moreover, in the following comparison with experiments will be carried out in the region of doping around the optimal one and in the overdoped regime where our approximation scheme reproduces the experimental findings of large Fermi surfaces satisfying Luttinger's theorem.[37]

With the use of the self-energy (3), the renormalized electron Green's function is then given by

$$G_\sigma(\mathbf{k}, i\omega) = [(G^I(\mathbf{k}, i\omega))^{-1} - \Sigma^p_\sigma(\mathbf{k}, i\omega)]^{-1}. \tag{6}$$

In Eq. (3) $D^0(\mathbf{q}, i\omega)$ is the unrenormalized Holstein phonon Green's function $D^0(\mathbf{q}, i\omega)=D^0(i\omega)$,

$$D^0(i\omega_n) = -\frac{\omega_0}{\omega_n^2 + \omega_0^2}. \tag{7}$$

Then Eq. (6) can also be rewritten as

$$G_\sigma(\mathbf{k}, i\omega) = [i\omega + \mu - \epsilon_{\mathbf{k}} - \Sigma^I_\sigma(i\omega) - \Sigma^p_\sigma(i\omega)]^{-1}, \tag{8}$$

where we have introduced

$$\Sigma^I_\sigma(i\omega) = \langle n_{-\sigma}\rangle U \frac{(i\omega+\mu)}{(i\omega+\mu) - (1-\langle n_{-\sigma}\rangle)U}. \tag{9}$$

The spectral function, which is measured in ARPES experiments, is related to the renormalized Green's function by the equation,

$$A_\sigma(\mathbf{k}, \omega) = -\frac{1}{\pi} \mathrm{Im}\, G_\sigma(\mathbf{k}, \omega) = -\frac{1}{\pi} \frac{\mathrm{Im}\, \Sigma^p_\sigma(\omega)}{\left(\dfrac{(\omega+\mu)^2 - (\omega+\mu)U}{(\omega+\mu) - U(1-\langle n_{-\sigma}\rangle)} - \epsilon_{\mathbf{k}} - \mathrm{Re}\, \Sigma^p_\sigma(\omega)\right)^2 + (\mathrm{Im}\, \Sigma^p_\sigma(\omega))^2}. \tag{10}$$

The quasiparticle dispersion is obtained, in the limit $\mathrm{Im}\,\Sigma^p(0)\to 0$, from the equation

$$\frac{(E_{\mathbf{k}}+\mu)^2-(E_{\mathbf{k}}+\mu)U}{(E_{\mathbf{k}}+\mu)-U(1-\langle n_{-\sigma}\rangle)}=\epsilon_{\mathbf{k}}+\mathrm{Re}\,\Sigma^p(E_{\mathbf{k}}), \tag{11}$$

where the index σ has been omitted for brevity. The excitation energy $E_{\mathbf{k}}$ is measured with respect to the renormalized chemical potential μ' which differs from the zeroth order chemical potential μ by the phononic correction $\mu'=\mu+\delta\mu$. The zeroth order chemical potential μ, which corresponds to the Hubbard-I solution, is determined by fixing the number of particles through the Green's function (4), while the correction $\delta\mu$ is given by the on-shell real part of the phonon self-energy, $\delta\mu=-\mathrm{Re}\,\Sigma^p(E_{\mathbf{k}}=0)$, which is determined through the Kramers-Kronig relation (14). Let us be reminded that $\mathrm{Im}\,\Sigma^p(i\omega)$ is zero within the energy range $\pm\omega_0$ where the quasiparticle peak is located. This guarantees absence of any singular contribution to $\delta\mu$ for $\omega\sim 0$. The correction to the zeroth order chemical potential is thus estimated to be very small (of the order of percent) due to the small value of the el-ph coupling g/W. Using Eqs. (3) and (4) the expression for the phonon contribution to the electron self-energy per spin is

$$\Sigma^p(i\omega)=\alpha\sum_{i=1,2}\int d\epsilon\rho_{2\mathrm{D}}(\epsilon)\Bigg\{\frac{A_i(\epsilon)}{i\omega-E_i(\epsilon)-\omega_0}[N_B(\omega_0)+1-N_F(E_i(\epsilon))]+\frac{A_i(\epsilon)}{i\omega-E_i(\epsilon)+\omega_0}[N_B(\omega_0)+N_F(E_i(\epsilon))]\Bigg\}, \tag{12}$$

where we have defined $\alpha=g^2/2W^2$ and N_B, N_F stand for the Bose and Fermi distribution functions,

$$E_{1,2}=\tfrac{1}{2}(U-2\mu+\epsilon\mp\sqrt{(U-\epsilon)^2+4U\epsilon\langle n_{-\sigma}\rangle}),$$

$$A_1(\epsilon)=\frac{E_1(\epsilon)-U(1-\langle n_{-\sigma}\rangle)}{E_1(\epsilon)-E_2(\epsilon)},\quad A_2(\epsilon)=1-A_1(\epsilon),$$

are the energies and spectral weights of the two Hubbard subbands. The density of states of a square lattice $\rho_{2\mathrm{D}}(\epsilon)$ with nearest neighbor transfer t_{ij} is given by the complete elliptic integral $(4/\pi^2)K(\sqrt{1-(2\epsilon/W)^2})$. Hereafter we use the bandwidth W as an energy unit. We further assume that the Coulomb interaction is sufficiently strong, so that the two Hubbard bands renormalized by phonon interaction do not overlap. Then from (12) we obtain the explicit expression for the imaginary part of the electron self-energy due to phonons

$$-\frac{1}{\alpha\pi}\mathrm{Im}\,\Sigma^p(\omega)=\rho_{2\mathrm{D}}\left(\frac{(\omega-\omega_0+\mu)^2-(\omega-\omega_0+\mu)U}{(\omega-\omega_0+\mu)-U(1-\langle n_{-\sigma}\rangle)}\right)\times[N_B(\omega_0)+1-N_F(\omega-\omega_0)]+\rho_{2\mathrm{D}}\left(\frac{(\omega+\omega_0+\mu)^2-(\omega+\omega_0+\mu)U}{(\omega+\omega_0+\mu)-U(1-\langle n_{-\sigma}\rangle)}\right)\times[N_B(\omega_0)+N_F(\omega+\omega_0)]. \tag{13}$$

The real part of the self-energy is then determined through the Kramers-Kronig relation:

$$\mathrm{Re}\,\Sigma^p(\omega)=\frac{1}{\pi}\int d\omega'\frac{\mathrm{Im}\,\Sigma^p(\omega')}{\omega'-\omega}. \tag{14}$$

II. ZERO TEMPERATURE ANALYSIS

To get some insights on the interplay of electron correlations and the electron-phonon interaction, we start by considering the zero temperature case. In this limit an analytic expression for the imaginary and real part of the self-energy can be inferred from Eqs. (13) and (14) by taking $U\to\infty$, $N_B(\omega_0)=0$, and $N_F(\omega)=1-\theta(\omega)$ and using the approximate expression for the DOS obtained by expanding around the Van Hove singularity (VHS)

$$\rho_{2\mathrm{D}}(\varepsilon)=\theta(1/2-|\varepsilon|)\frac{4}{\pi^2}K(\sqrt{1-(2\varepsilon)^2})\simeq\theta(1/2-|\varepsilon|)\frac{4}{\pi^2}(-\ln|\varepsilon|+C), \tag{15}$$

where $C=3/2\ln 2$. This expansion substituted into (14) yields a lengthy expression. Below we give the contribution coming from the constant term in (15),

$$\mathrm{Re}\,\tilde{\Sigma}^p(\omega)=-\frac{4\alpha}{\pi}C\int_{-\infty}^{\infty}d\omega'\Bigg\{\frac{\theta(\omega'-\omega_0)}{\omega'-\omega}\theta\Bigg(\frac{1-\langle n_{-\sigma}\rangle}{2}-|\omega'+\mu-\omega_0|\Bigg)+\frac{\theta(-\omega'-\omega_0)}{\omega'-\omega}\theta\Bigg(\frac{1-\langle n_{-\sigma}\rangle}{2}-|\omega'+\mu+\omega_0|\Bigg)\Bigg\}, \tag{16}$$

which results in

$$-\frac{\pi}{4\alpha C}\mathrm{Re}\,\tilde{\Sigma}^p(\omega)=\ln\left|\frac{\omega+\omega_0}{\omega-\omega_0}\right|+\ln\left|\frac{\omega-\left(\omega_0+\frac{1-\langle n_{-\sigma}\rangle}{2}-\mu\right)}{\omega+\left(\omega_0+\frac{1-\langle n_{-\sigma}\rangle}{2}+\mu\right)}\right|. \tag{17}$$

From Eq. (17) it is seen that $|\mathrm{Re}\,\Sigma^p(\omega)|$ has four logarithmic singularities. For an infinite band, and in absence of electron correlations, only the first term of (17) survives that corresponds to the classical result of Ref. 38. In this case the singularities occur at $\pm\omega_0$ and two shoulders appear at energies $\omega>\omega_0$ and $\omega<-\omega_0$. Such a simple expression of $\mathrm{Re}\,\Sigma^p$ has been recently taken into consideration in Ref. 24 to interpret the unusual isotope shift in the real part of the self-energy in the optimally doped Bi2212.[9] But the calculations presented in Ref. 24 do not contain information on the electron correlations and on finite bandwidth which are important in the interpretation of the experimental findings. The effect of finite bandwidth on the spectrum in absence of Cou-

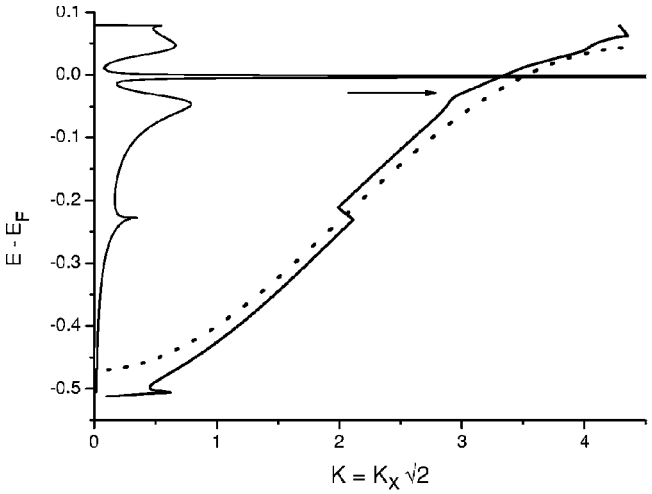

FIG. 1. Spectral density function at $\varepsilon(k)=0.35$ and dispersion along the diagonal direction for $\alpha=0.02$ (thick continuous line) and $\alpha=0$ (dotted line) for $\omega_0=0.035$, $T=0.005$, $U=3$, $\delta=0.05$. All the energies are in units of bandwidth W. Momentum is along the diagonal direction Γ-Y of the Brillouin zone. The arrow indicates the kink position.

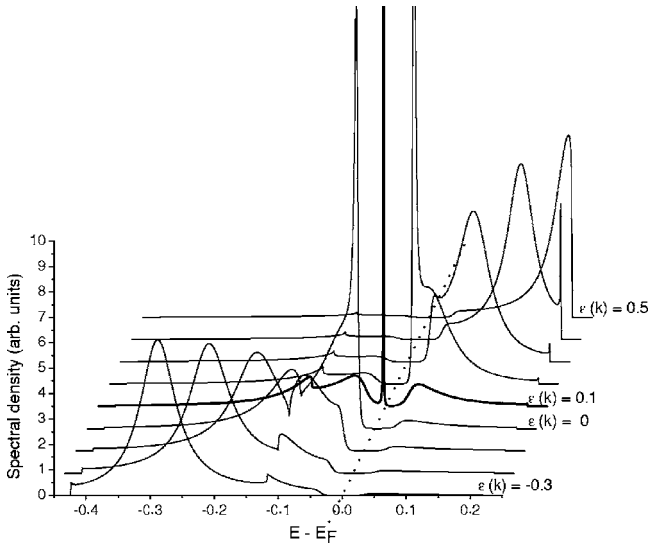

FIG. 2. Energy distribution curves for different values of the momentum along the diagonal [$\varepsilon(k)$ is the bare electron dispersion]. The parameters are: $\alpha=0.02$, $\omega_0=0.035$, $T=0.004$, $U=3$, $\delta=0.15$ (optimal doping).

lomb interactions has recently been considered in Ref. 39 where an additional singularity due to band edges has been found. As can be seen from (17) in the presence of electron correlations this singularity becomes strongly dependent on doping compared to Ref. 39. In our treatment an additional dilogarithmic singularity of the $\mathrm{Re}\,\Sigma^p$ appears due to the VHS in the density of states. We will show below that the doping dependence is the ingredient that permits us to explain some experimental features of the quasiparticle dispersion that are lacking in previous calculation schemes.

III. NUMERICAL RESULTS

In the following we present the numerical results for the quasiparticle dispersion and the spectral intensity taking into account both the effect of the two-dimensional lattice density of states and the reduction of electronic spectral weight at low energies due to strong electron correlations.

As already mentioned, the parameters have been scaled with the bandwidth W. Assuming the hopping integral $t=0.25$ eV, we have $W=2$ eV. Thus the phonon frequency $\omega_0=70$ meV after scaling becomes $\omega_0=0.035$, and the temperature $T=100\ \mathrm{K}\rightarrow T=0.004$. The standard definition of the electron-phonon coupling constant is $\lambda=[2N(0)/\omega_0]\alpha$ which includes the density of states at the Fermi energy and is thus concentration dependent, therefore in the following we use the quantity α. λ is usually determined in an indirect way from experimental data, e.g., from the slope of the quasiparticle dispersion.[27] In particular, for Pb $\lambda=2$ and if we take a simple estimate for the density of states at the Fermi level, $N(0)\simeq 1/W=0.5\ (\mathrm{eV})^{-1}$, then the coupling constant α is 0.035.

A. Quasiparticle line-shape and spectrum

In Fig. 1 we show the dispersion along the diagonal direction $\Gamma(0,0)-Y(\pi,\pi)$ of the Brillouin zone as given by solution of Eq. (11) together with the spectral density function. The main features of the DOS are the central peak corresponding to the quasiparticle (QP) excitation and the two incoherent humps above and below E_F corresponding to phonon emission. The fine structures at high energies are related to band edges and to the logarithmic VHS present in the lower energy hump at $E-E_F\sim-0.25$. The dip structure at $\sim\pm\omega_0$ originates from the logarithmic singularity in Eq. (17) at zero temperature. Comparison with the dotted curve corresponding to $\alpha=0$ clearly shows a significant modification of high energy spectrum when states are created above and below the band edges.[39] Decreasing the momentum, the spectral weight is transferred from the upper hump and from the QP peak to the lower hump, until the QP and the dip structure disappear as shown in Fig. 2. This behavior has been recently observed in photoemission experiments.[3,9] As follows from our analysis of the spectral density in Fig. 2, the dispersion at $E-E_F<-\omega_0$ in Fig. 1 corresponds to a broad peak (hump). As can be seen from Fig. 1, the kink (indicated by arrow in the figure) appears as a change of slope of the two straight lines, the upper line corresponding to the QP dispersion branch and the lower one corresponding to the higher energy hump. Although the two branches are disconnected by the logarithmic singularity we choose to interpolate them with a continuous line to make a direct connection to experiments. In experiments the dispersion curve looks continuous due to large amount of extraneous damping not included in our theory and the kink is determined by the crossing of two straight lines corresponding to the low-energy and high-energy dispersion branches. The energy drop we observe at momentum around $k\sim 2$ is due to VHS. After crossing this momentum the QP switches to a new dispersion branch, leaving behind a nondispersive weak peak at the energy corresponding to VHS. Note that at the electron concentration considered the QP renormalized by phonons

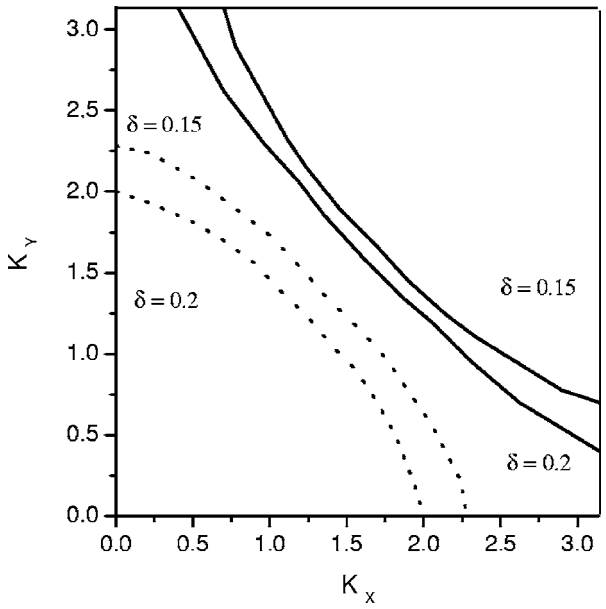

FIG. 3. Fermi surface (continuous line) and locus of kink momenta (dotted line) in the first Brillouin zone for the hole doping $\delta=0.15$ and $\delta=0.2$, while the other parameters are: $\alpha=0.04$, $\omega_0=0.04$, $T=0.006$, $U=2$.

has a linear dispersion while the dispersion of the correlated electron with $\alpha=0$ is nonlinear around E_F (see dotted line).[40] In Fig. 3 we show the evolution of the Fermi surface (FS) and the locus of the kink momenta in the Brillouin zone for different values of the doping ($\delta=0.15$ and $\delta=0.2$, the other parameters are reported in the caption). An interesting feature is that while the FS is holelike the locus of the kink momenta is electronlike. This agrees with the experimental findings in $Bi_2Sr_2CaCu_2O_8$ around optimal doping.[41] The locus of the kink position below the FS corresponds to the emission of a phonon of fixed frequency. Since the energy separation between the FS and the kink surface is around ω_0, the difference in topology is due to a significant flattening of the QP dispersion in the direction close to the $(\pi,0),(0,\pi)$ line compared to the diagonal. This effect depends on doping, and is found around optimal doping. In the underdoped and overdoped regimes we find that both surfaces are either holelike or electronlike.

B. Doping dependence

In Fig. 4 we show the quasiparticle dispersion as function of doping for the values of the parameters reported in the caption. For each curve the kink position is determined by the crossing of the two straight lines corresponding to the QP and to the high-energy hump. The evolution of the kink position with hole doping along the diagonal is very close to the one observed experimentally.[9,10] At $\delta=0.15$ we find the position of the kink at $k_x\simeq 0.47$ (in unit of π/a, $a=1$ being the lattice constant) while the experimental value is about $k_x\simeq 0.37$ to $k_x\simeq 0.39$.[9] An estimation of the kink momentum closer to the experimental value is obtained by the inclusion of next-nearest neighbor (n.n.n.) hopping. Indeed for the choice of the n.n.n. hopping $t'/t=-0.4$ the kink position

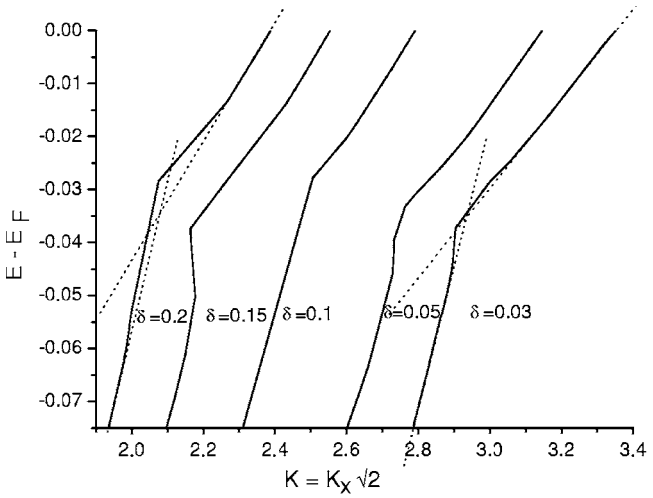

FIG. 4. Dispersion $E(k)$ at different dopings for $\omega_0=0.035$, $\alpha=0.02$, $U=3$, $T=0.003$. The kink position is determined by the crossing of the two straight lines corresponding to the QP branch and to the high-energy hump.

along the diagonal is moved to $k_x=0.4$, in better agreement with experiments.

An important feature shown by our results, and also observed in experiments,[3,14] is that the quasiparticle velocity ratio[27] $R_v\equiv v(\omega>\omega_{\rm kink})/v(\omega<\omega_{\rm kink})$ (where v is given by the slope of the curve) changes most rapidly at low doping and reaches saturation close to optimal doping ($\delta>0.1$), i.e., the kink becomes smoother with doping. The dependence of R_v on doping in our description is due to the correlated nature of the bare electron band. Indeed, in the interval $\delta<0.1$ the Fermi energy is close to the top of the band where the correlated electron spectrum with $\alpha=0$ is nonlinear (see dotted line in Fig. 1) in good agreement with QMC calculations.[40] Inclusion of the el-ph interaction induces a linear dispersion close to E_F (Ref. 24) whose slope in our approach depends on doping. This gives a concentration dependent phonon effect. At larger doping, $0.1<\delta<0.25$ the Fermi energy falls within the linear region of the correlated electron dispersion independent from doping, i.e., the slope becomes constant and the effect of phonons is almost independent from concentration. In contrast, the high energy features, or humps, remain strongly dependent on doping. Of course, in experiments it is difficult to extract the purely electronic dispersion and the nonlinear behavior around E_F at low-doping is not directly observable, anyway such nonlinearity could provide an explanation of the doping dependent kink features. For the parameters chosen in the Fig. 1 we find that $R_v\simeq 2.17$ for $\delta=0.15$ and $R_v\simeq 3.15$ for $\delta=0.03$. These values are close to the experimental ones. The parameter $\alpha=0.02$ we have chosen in Fig. 4 corresponds to the coupling constant $\lambda=1.14$, suggesting that the system is in the intermediate coupling regime.

C. Temperature dependence and isotope effect

Other properties which can be explained within the phonon scenario are related to the changes in temperature and on

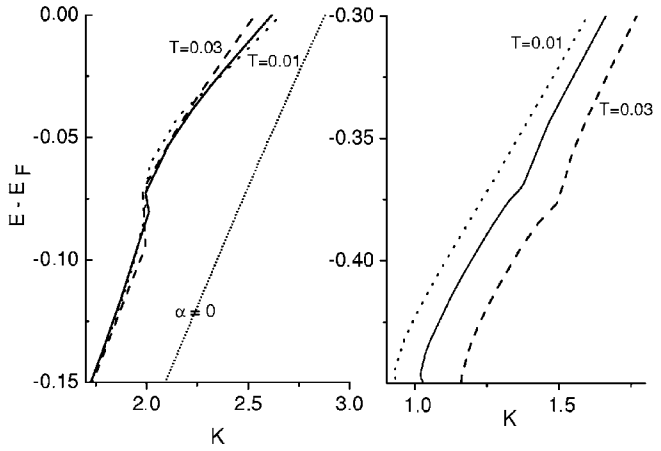

FIG. 5. Left panel: Dispersion $E(k)$ close to the Fermi energy at different temperatures, $T=0.01$, 0.02, 0.03 for $\delta=0.1$, $\omega_0=0.05$, $U=3$, $\alpha=0.05$. Right panel: Dispersion at energy larger than the kink (for the same parameters). The biggest changes with temperature due to phonons are observed away from the kink position in a broad temperature range.

isotope substitution observed in the experimental spectra, which occur at energies much larger than ω_0. In Fig. 5 we show the temperature dependence of the energy dispersion close to the kink position (left panel) and at higher energies (right panel). The energy of the kink is only slightly increasing with T and the kink is smoothed. The main dependence on temperature is instead observed away from the kink region.

Regarding the isotope effect, it has been experimentally observed both in the coherent (peak) and incoherent (hump) parts of the spectrum.[9] Comparison between the O^{16} and O^{18} dispersions in experiments shows that the kink separates the low-energy regime, where the spectrum shows a coherent peak and negligible isotope effect, from the high-energy regime where the spectrum is more incoherent and shows appreciable isotope effect. In Fig. 6 we report the low energy dispersion for two different isotope values of ω_0, 0.03 and 0.035, while keeping the value of $\lambda=[2N(0)/\omega_0]\alpha$ fixed. We

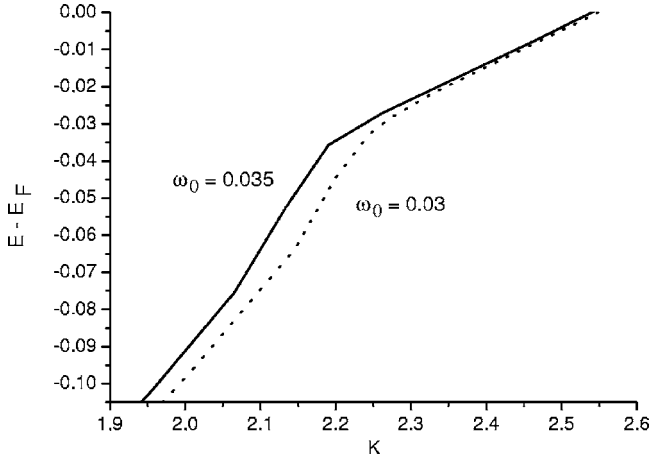

FIG. 6. Isotope effect in the quasiparticle dispersion at $T=0.004$ for $\delta=0.15$, $U=3$, $\lambda=1$.

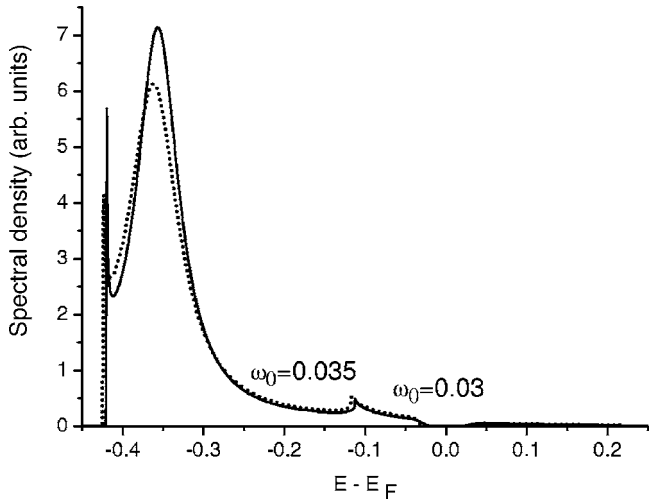

FIG. 7. Isotope effect in the spectral density function at $T=0.004$ for $\varepsilon(k)=-0.4$, $U=3$, $\delta=0.15$, $\lambda=1$.

find a significant isotope effect below the kink $E-E_F<-\omega_0$ where the heavier isotope (smaller ω_0) has a lower dispersion in agreement with experiments, while no isotope effect is observed in the low energy regime. In Fig. 7 we report the spectral intensity for the values of the parameters as in the EDC curve N.5 in Ref. 9. The intensity presents a broad maximum at higher energy that corresponds to a dispersive "overdamped QP"[9] and a nondispersive weak peak at lower energy. There is a considerable isotope dependent redistribution of spectral weight and energy shift of the main peak. For the heavier isotope material more spectral weight is transferred to lower energies as compared to the lighter isotope, in agreement with experimental results. The isotope effect in the incoherent part of the spectrum is also a characteristic of the EDC curves obtained in experiments. The isotope shift is reduced by temperature. The isotope effect at the phonon frequency and above it would not be reproduced in a model without electron correlations that induce a doping dependent redistribution of spectral weight at high energy.

IV. CONCLUSIONS

We have analyzed the effect of electron correlations on the energy spectra of the electrons coupled to the Einstein phonon in the two-dimensional Hubbard model. The doping, temperature dependence, and isotope effect of the spectral intensity and of the energy dispersion along the diagonal direction of the Brillouin zone are in good agreement with recent experiments in the normal state of high-T_c cuprates. The spectral intensity presents a characteristic peak/dip/hump structure in which the dip corresponds to the phonon frequency while a kink appears in the dispersion at the same energy as the dip. The spectrum for the correlated electrons interacting with Einstein phonons contains two branches, a renormalized quasiparticle branch, for energies below the phonon frequency, and a dispersive branch (hump) for larger energy. Following experiments, we determine the kink position by the crossing of two straight lines corresponding to the two branches. Close to optimal doping, the locus of the kink

position in the Brillouin zone is found to be electronlike while the Fermi surface is holelike in agreement with experiments. The spectral intensity and the electron dispersion are found to be strongly dependent on temperature, doping, and isotope substitution especially at energies much larger then the phonon frequency. We have shown that the effect of electron correlations becomes evident in the doping dependence of the energy dispersion and line shape. In particular, our results qualitatively reproduce recent experiments which show a significant change in the ratio of the slopes (or velocities) of the kink structure at low doping which saturates close to optimal doping. Such dependence can be understood if one notes that at low doping the Fermi energy is located in the nonlinear region of the correlated electron spectrum, which becomes linear due to the interaction with phonons but acquiring a doping dependent slope. We find that for doping larger than $\delta \sim 0.1$ the Fermi energy is located in the linear part of the correlated electron spectrum (doping independent). The dependence on doping disappears and the velocity ratio saturates. In contrast, the high energy features of the spectrum remain dependent on doping. Finally, we have analyzed the effect of isotope substitution that consists of redistribution of the spectral weight at low energies and in the energy shift of the humps in agreement with experiments. We would like to mention that our analysis can also be applied to the study of the photoabsorption regime where a similar behavior for the electronlike excitations is expected. The approximation we have used to describe strongly correlated electrons is just the simplest possible one and further refinements could account for more realistic features, for example, including a realistic electronic band structure, dynamical effects, anisotropy, and momentum dependence of phonon coupling.[42] Work is in progress along this direction. Nevertheless, the good qualitative agreement with a number of recent experiments suggests that strong electron correlations are crucial for understanding the role of phonons in high-T_c superconductors.

[1] A. Damscelli, Z. Hussain, and Z.-X. Shen, Rev. Mod. Phys. **75**, 473 (2003).

[2] J. C. Campuzano, M. R. Norman, M. Randeria, in *Physics of Superconductors*, edited by K. H. Bennemann and J. B. Ketterson (Springer, Berlin, 2004), Vol. II, pp. 167–273.

[3] A. Lanzara, P. V. Bogdanov, X. J. Zhou, S. A. Kellar, D. L. Feng, E. D. Lu, T. Yoshida, H. Eisaki, A. Fujimori, K. Kishio, J.-I. Shimoyama, T. Noda, S. Uchida, and Z. Hussain, Nature (London) **412**, 510 (2001).

[4] S. V. Borisenko, A. A. Kordyuk, T. K. Kim, A. Koitzsch, M. Knupfer, J. Fink, M. S. Golden, M. Eschrig, H. Berger, and R. Follath, Phys. Rev. Lett. **90**, 207001 (2003); A. D. Gromko, A. V. Fedorov, Y. -D. Chuang, J. D. Koralek, Y. Aiura, Y. Yamaguchi, K. Oka, Yoichi Ando, and D. S. Dessau, Phys. Rev. B **68**, 174520 (2003).

[5] T. K. Kim, A. A. Kordyuk, S. V. Borisenko, A. Koitzsch, M. Knupfer, H. Berger, and J. Fink, Phys. Rev. Lett. **91**, 167002 (2003).

[6] T. Sato, H. Matsui, T. Takahashi, H. Ding, H.-B. Yang, S.-C. Wang, T. Fujii, T. Watanabe, A. Matsuda, T. Terashima, and K. Kadowaki, Phys. Rev. Lett. **91**, 157003 (2003).

[7] A. Lanzara, P. V. Bogdanov, X. J. Zhou, N. Kaneko, H. Eisaki, M. Greven, Z. Hussain, and Z. -X. Shen, cond-mat/0412178.

[8] P. D. Johnson, T. Valla, A. V. Fedorov, Z. Yusof, B. O. Wells, Q. Li, A. R. Moodenbaugh, G. D. Gu, N. Koshizuka, C. Kendziora, Sha Jian, and D. G. Hinks, Phys. Rev. Lett. **87**, 177007 (2001).

[9] G.-H. Gweon, T. Sasagawa, S. Y. Zhou, J. Graf, H. Takagi, D.-H. Lee, and A. Lanzara, Nature (London) **430**, 187 (2004).

[10] G.-H. Gweon, S. Y. Zhou, and A. Lanzara, J. Phys. Chem. Solids **65**, 1397 (2004).

[11] H. F. Fong, B. Keimer, P. W. Anderson, D. Reznick, F. Dogan, and I. A. Aksay Phys. Rev. Lett. **75**, 316 (1995).

[12] P. Bourges, Y. Sidis, H. F. Fong, L. P. Regnault, J. Bossy, A. Ivanov, and B. Keimer, Science **288**, 1234 (2000).

[13] A. Kaminski, M. Randeria, J. C. Campuzano, M. R. Norman, H. Fretwell, J. Mesot, T. Sato, T. Takahashi, and K. Kadowaki, Phys. Rev. Lett. **86**, 1070 (2001).

[14] X. J. Zhou, T. Yoshida, A. Lanzara, P. V. Bogdanov, S. A. Kellar, K. M. Shen, W. L. Yang, F. Ronning, T. Sasagawa, T. Kakeshita, T. Noda, H. Eisaki, S. Uchida, and C. T. Lin, Nature (London) **423**, 398 (2003).

[15] T. Cuk, F. Baumberger, D. H. Lu, N. Ingle, X. J. Zhou, H. Eisaki, N. Kaneko, Z. Hussain, T. P. Devereaux, N. Nagaosa, and Z.-X. Shen, Phys. Rev. Lett. **93**, 117003 (2004).

[16] T. P. Devereaux, T. Cuk, Z. X. Shen, and N. Nagaosa, Phys. Rev. Lett. **93**, 117004 (2004).

[17] X. J. Zhou, Junren Shi, T. Yoshida, T. Cuk, W. L. Yang, V. Brouet, J. Nakamura, N. Mannella, Seiki Komiya, Yoichi Ando, F. Zhou, W. X. Ti, J. W. Xiong, Z. X. Zhao, T. Sasagawa, T. Kakeshita, H. Eisaki, S. Uchida, A. Fujimori, Zhenyu Zhang, E. W. Plummer, R. B. Laughlin, Z. Hussain, and Z.-X. Shen, Phys. Rev. Lett. **95**, 117001 (2005).

[18] H. Keller, Physica B **326**, 283 (2003), and references therein.

[19] J. H. Kim, K. Levin, R. Wentzcovitch, and A. Auerbach, Phys. Rev. B **44**, 5148 (1991); J. H. Kim and Z. Tesanovic, Phys. Rev. Lett. **71**, 4218 (1993).

[20] Z. B. Huang, W. Hanke, E. Arrigoni, and D. J. Scalapino, Phys. Rev. B **68**, 220507(R) (2003).

[21] E. Cappelluti, B. Cerruti, and L. Pietronero, Phys. Rev. B **69**, 161101(R) (2004).

[22] E. Koch and R. Zeyher, Phys. Rev. B **70**, 094510 (2004).

[23] R. Citro and M. Marinaro, Eur. Phys. J. B **20**, 343 (2001).

[24] E. G. Maksimov, O. V. Dolgov, and M. L. Kulic, cond-mat/0408251.

[25] G. Sangiovanni, M. Capone, C. Castellani, and M. Grilli, Phys. Rev. Lett. **94**, 026401 (2005).

[26] W. Koller, D. Meyer, and A. C. Hewson, Phys. Rev. B **70**, 155103 (2004); W. Koller, A. C. Hewson, and D. M. Edwards, cond-mat/0508463 (unpublished).

[27] S. Ishihara and N. Nagaosa, Phys. Rev. B **69**, 144520 (2004).

[28] O. Rosch and O. Gunnarsson, Phys. Rev. Lett. **92**, 146403 (2004).

[29] A. S. Mishchenko and N. Nagaosa, Phys. Rev. Lett. **93**, 036402 (2004).
[30] M. Eschrig and M. R. Norman, Phys. Rev. B **67**, 144503 (2003).
[31] A. W. Sandvik, D. J. Scalapino, and N. E. Bickers, Phys. Rev. B **69**, 094523 (2004).
[32] J.-X. Li, T. Zhou, and Z. D. Wang, cond-mat/0501356.
[33] J. Hubbard, Proc. R. Soc. London, Ser. A **276**, 238 (1963).
[34] M. I. Vladimir and V. A. Molskalenko, Theor. Math. Phys. **82**, 301 (1990); V. A. Moskalenko and L. Z. Kon, Condens. Matter Phys. **1**, 23 (1998).
[35] W. Metzner, Phys. Rev. B **43**, 8549 (1991).
[36] A. Georges, G. Kotliar, W. Krauth, and M. J. Rozenberg, Rev. Mod. Phys. **68**, 13 (1996).
[37] C. Gröber, R. Eder, and W. Hanke, Phys. Rev. B **62**, 4336 (2000); A. Dorneich, M. G. Zacher, C. Gröber, and R. Eder, cond-mat/9909352; J. Zielinski, M. Mierzejewski, and P. Entel, Phys. Rev. B **57**, 10311 (1998).
[38] S. Engelsberg and J. R. Schrieffer, Phys. Rev. **131**, 993 (1963).
[39] F. Dogan and F. Marsiglio, Phys. Rev. B **68**, 165102 (2004).
[40] N. Bulut, D. J. Scalapino, and S. R. White, Phys. Rev. B **50**, 7215 (1994).
[41] P. V. Bogdanov, A. Lanzara, S. A. Kellar, X. J. Zhou, E. D. Lu, W. J. Zheng, G. Gu, J.-I. Shimoyama, K. Kishio, H. Ikeda, R. Yoshizaki, Z. Hussain, and Z. X. Shen, Phys. Rev. Lett. **85**, 2581 (2000).
[42] T. P. Devereaux, T. Cuk, Z.-X. Shen, and N. Nagaosa, Phys. Rev. Lett. **93**, 117004 (2004).